

Phenomenological Model of the Nonlinear Microwave Response of a Superconducting Weak Link

Anton V. Velichko^{1,2}

¹School of Electronic & Electrical Engineering, University of Birmingham, UK

²Institute of Radiophysics & Electronics of NAS, Ukraine

A phenomenological model is proposed which describes the effect of both dc and rf magnetic fields, H , on the microwave surface impedance, $Z_s = R_s + jX_s$, of a superconducting weak link. Two cases are considered; a weak link between two grains, shunted by another grain, and a non-shunted weak link. In both cases, the dependences of R_s and X_s on applied H were found to be non-monotonic. Under certain conditions, the values of $Z_s(H)$ can fall below the zero-field values. The application of the model to describe recent experimental results on $Z_s(H)$ is briefly discussed.

Microwave breakdown, being one of the most fascinating phenomenon of the contemporary physics of superconductivity, is not yet fully understood. A few simple phenomenological models¹⁻³ developed recently have helped to shed some light on the mechanisms of the microwave nonlinearity in high-temperature superconductors (HTS). However, in the last few years, there have appeared some observations of quite unusual features in both the rf and dc field dependences of the microwave surface impedance, $Z_s = R_s + jX_s$. Both the surface resistance, R_s , and the surface reactance, X_s , were reported to change non-monotonously with field in epitaxial HTS thin films.⁴⁻⁷ Here, the values of R_s and X_s in applied fields, H were sometimes seen to fall below the relevant zero-field values. Several hypotheses have been put forth to explain these peculiarities in $Z_s(H)$. Among them are stimulation of superconductivity^{5,6,8}, and field-induced alignment of magnetic impurity spins.^{4,6,9} However, until now no theoretical model of $Z_s(H)$ incorporating the above mentioned scenarios has been proposed. At the same time, a phenomenological model, recently developed by Gallop et al.¹⁰ to explain the difference in the effect of dc and rf magnetic fields upon Z_s , was surprisingly found to give a reduction of the microwave losses (R_s) with increased field. In that model, the microwave response of a Josephson weak link (WL) shunted by a superconducting grain was considered. However, no reduction of X_s with the field can be obtained within the framework of Gallop's model, saying nothing about correlating decrease of both $R_s(H)$ and $X_s(H)$ (for the argumentation see discussion of the results), as it was experimentally observed by some groups^{4,7}.

In the present paper, we present a unified model for the microwave response of a superconducting WL, considered as a Josephson tunnel Junction (JTJ). The surrounding grains and the WL itself are modelled by an equivalent circuit, the elements of which, resistivities and conductivities, represent dissipative and inertial processes in the

structure. Two cases are considered. Firstly, a simple WL between two grains. Secondly, WL shunted by another third grain¹¹, which is strongly coupled to the other two grains. These two topologies are hereafter referred to as "the non-shunted" and "the shunted WL geometry", respectively. The second geometry was previously considered by Gallop et al.¹⁰, using the effective medium approach¹², when the Josephson penetration depth, λ_J is a function of the average grain size, a . The above approach, however, is justified only if $\lambda_J \gg a$.

The main assumption of this paper is that for high-quality HTS films, due to high critical current densities, J_c (in excess of 10^6 A/cm²), and larger grain sizes (up to several μm), the effective medium approach breaks down, and the films have to be considered as an array of long Josephson junctions (JJ). In this case, λ_J is no longer dependent on a , but rather depends on the magnetic thickness of the junction, $d_m = 2\lambda_L + d$; here, λ_L and d are the London penetration depth and the grain separation, respectively. Another important feature of the model presented here is that for the non-shunted WL geometry, we consider a limit of $\lambda_J \leq a$. This brings about the appearance of a size effect in the junction resistivity, ρ_J , which manifests itself as a maximum in $\rho_J(H)$, when λ_J is varied with increasing H . Under certain conditions, the assumptions made above may lead to appearance of non-monotonic behavior or decrease in $R_s(H)$ and $X_s(H)$. These results are compared favorably with recent microwave experiments on HTS thin films.

The model presented here is based on the equivalent circuit description of superconductors.¹³ The general equivalent circuit, comprising both the situations modelled in the present paper, is shown in Fig. 1. The effective complex resistivity of the grains, according to Fig. 1, in the limit of $\rho_{s1} \gg \omega l_g$ (which is always valid for $f \leq 100$ GHz and temperatures not too close to the critical temperature, T_c), can be written as

$$\rho_g^{eff} = \rho_{g1} + j \cdot \rho_{g2} \simeq \frac{(\omega l_s)^2}{\rho_{s1}} + j\omega l_s. \quad (1)$$

Note that in the above limit, $l_g = l_s$; here, l_g and l_s are the effective and the real grain inductivity, respectively. A straightforward conclusion which immediately follows from the form of Eq.(1), is that the effective medium parameters, ρ_{g1} and ρ_{g2} , are included *in series*, whereas the initially used real medium parameters, ρ_{s1} and l_s , were included *in parallel*!

The main assumptions of the model are as follows. The magnetic field (rf and dc) affects the critical current den-

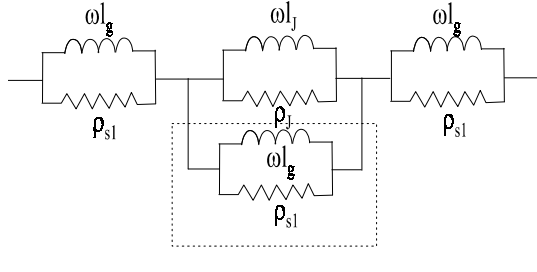


FIG. 1. Equivalent circuit of a grain-shunted weak link. In the case of the non-shunted weak link, the part of the circuit surrounded by the dashed rectangle is absent.

sity of the junction, J_c , and the bulk (grain) penetration depth, λ_g . Both rf and dc fields are assumed to act in the same way. Both rf and dc current densities, J_{rf} and J_{dc} , associated with applied rf and dc fields, are assumed to be smaller than J_c . Within the whole range of the applied field, grains are assumed to be in the Meissner state. However, nonlinear dissipation arises within the grains due to pair breaking produced by the rf current. Here, the field dependence of λ_g is described by the Ginzburg-Landau theory¹⁴

$$\lambda_g = \frac{\lambda_g(0)}{\sqrt{(1 - \alpha(H/H_c)^2)}} = \frac{\lambda_g(0)}{\sqrt{(1 - (H/H_g)^2)}} \quad (2)$$

where α can be found from the Ginzburg-Landau theory. To simplify the simulation, we have merged all the pre-factors of H^2 into one, which we called “the grain scaling field”, $H_g = 2H_c/\sqrt{\alpha}$. From Eq.(1) it follows that the real part of ρ_g^{eff} is given by

$$\rho_g = \frac{(\omega l_g)^2}{\rho_{s1}(0)(1 + (H/H_g)^2)}, \quad (3)$$

where $\rho_{s1}(0)$ is a low field quasiparticle resistivity. Here, again the Ginzburg-Landau type of the nonlinearity is assumed. The field dependence of the critical current of a JTJ is given by¹⁵

$$I_c = I_{c0} \cdot \frac{\sin(\pi\Phi/\Phi_0)}{\pi\Phi/\Phi_0} \sim I_{c0} \cdot \frac{\sin(H)}{H}. \quad (4)$$

However, this dependence holds only for a uniform junction of rectangular shape. In a real junction, the effects of the shape and the transport current self-field lead to severe distortion (skewing) of the above dependence, with the oscillation peaks being smeared out (especially noticeable in a long junction with length $L \gg \lambda_J$).¹⁵ Therefore, instead of (4), we use its envelope, which we believe is a good qualitative approximation for $J_c(H)$ of a long, non-rectangular junction, and is given by

$$J_c = J_{c0} \cdot \frac{1}{1 + H/H_J}, \quad (5)$$

where H_J is the junction scaling field ($\sim H_{c1J}$, the junction lower critical field). According to Mahel et al.¹⁶,

Eq.(5) will also hold for an ensemble of JJs with a random distribution of critical currents and dimensions.

The Josephson penetration depth of a JTJ is described as (see, e. g., Ref.¹⁵)

$$\lambda_J = \sqrt{\frac{\hbar}{2e\mu_0 J_c d_m}}. \quad (6)$$

From simple geometrical considerations, we can easily work out the junction resistivity, which for cubic grains of size $a \gg \lambda_J$ is represented as

$$\rho_J = R_n \frac{4\lambda_J(a - \lambda_J)}{d}, \quad (7)$$

where R_n is the junction normal resistance. The inductivities of the grains and the junction are given by

$$l_g = \omega \lambda_g^2, \quad l_J = \omega \lambda_J^2. \quad (8)$$

Finally, the total effective resistivity of the junction is

$$\rho_{eff} = (\rho_g + j\omega l_g) + \left[\frac{1}{\rho_g + j\omega l_g} + \frac{1}{\rho_J} + \frac{1}{\omega l_g} \right]^{-1}. \quad (9)$$

This expression is valid for the shunted WL geometry. For the case of the non-shunted junction, the first term in the square brackets of Eq.(9) has to be omitted. In addition, for the shunted WL geometry, a part of the transport current (both rf and dc) will flow through the shunting grain. Therefore, additional weighting factors have to be introduced in the expressions for the grain penetration depth, Eq.(1), and the junction critical current, Eq.(4). For rf current, in the case of $\rho_J \gg \omega l_J$ considered in this paper, these factors are

$$\alpha_J = \frac{l_g}{l_g + l_J}, \quad \alpha_g = \frac{l_J}{l_g + l_J}, \quad (10)$$

where indexes “g” and “J” denotes grains and junction, respectively. For dc currents, these factors will be different, but here we shall not consider the case of a dc field for the shunted junction geometry.

Finally, the surface impedance of the whole structure is

$$Z_s^{eff} = \sqrt{j\omega\mu_0\rho_{eff}}. \quad (11)$$

For the non-shunted weak link geometry, we consider the limit when $a \geq \lambda_J$ ($\lambda_J > \lambda_g$ always holds).¹⁷ As will be shown later, in this limit a non-monotonic behavior of $R_s(H)$ and $X_s(H)$ may be observed under certain conditions. The field dependences of R_s and X_s , with R_n as a variable parameter, are shown in Fig. 2. Other parameters are chosen in such a way that at low R_n , $\omega l_g \ll \rho_J \ll \omega l_J$. As we can see, at the lowest R_n -value [Figs. 2 (a), 2(b)], both $R_s(H)$ and $X_s(H)$ increase at low fields, then pass through a maximum, and eventually decrease with increased H . Here, the maximum in $R_s(H)$ is broader and shifted to higher H than

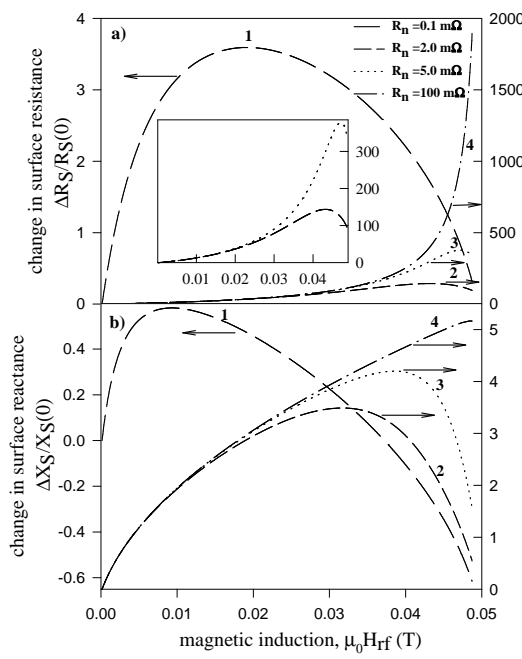


FIG. 2. Magnetic field, H , dependence of the change in the surface resistance, $\Delta R_s = R_s(H_{rf}) - R_s(0)$, and the surface reactance, $\Delta X_s = X_s(H_{rf}) - X_s(0)$, normalized by their low-field values, $R_s(0)$ and $X_s(0)$, for the non-shunted weak link for different R_n values (given in the figures). Other parameters of the simulation are as follows: $f = 8 \cdot 10^9$ Hz; $\lambda_g(0) = 1.4 \cdot 10^{-7}$ m; $\rho_{s1}(0) = 2 \cdot 10^{-6}$ Ω·m; $J_{c0} = 1 \cdot 10^9$ A/m²; $H_J = 9.2 \cdot 10^2$ A/m; $H_g = 6.4 \cdot 10^6$ A/m; $d = 2 \cdot 10^{-8}$ m; $a = 6.1 \cdot 10^{-6}$ m. The inset shows curves 2 and 3 on an expanded scale.

that in $X_s(H)$. With increased R_n , the maxima shift to higher fields. Here, the peak in $R_s(H)$ becomes narrower, and eventually disappears at high R_n . A similar transformation occurs with $X_s(H)$, except that at the highest R_n (100 mΩ), $X_s(H)$ gains a curvature opposite to that of $R_s(H)$ (downward and upward, respectively). It should be noted that for the lowest R_n , both $R_s(H)$ and $X_s(H)$ decrease simultaneously over a sufficiently broad field range (~ 30 mT).

In the geometry of the shunted weak link only the case of rf-field dependence of Z_s is considered, with weighting factors for rf-current given by Eq.(10), which is valid in the limit when $\rho_J \gg \omega l_J$. The only variable parameter in this case is, again, R_n . A remarkable feature of this geometry is that at low R_n , $R_s(H)$ may decrease monotonously starting from the lowest fields, being accompanied by sublinear ($\sim H^n$, $n < 1$) increase of $X_s(H)$ [Fig. 3 (a), 3 (b)]. At higher R_n , there is a maximum in $R_s(H)$, which shifts to higher fields with increased R_n . Eventually, $R_s(H)$ translates into a sublinear function of H , similar to $X_s(H)$ (Fig. 4). It should be noted that with the change in R_n , no noticeable transformation occurs to $X_s(H)$, which preserves not only the functional form, but even the absolute values.

The non-monotonic behavior in $Z_s(H)$ for the two geometries has different origins. In the case of the non-shunted WL, all the peculiarities in $R_s(H)$ and $X_s(H)$

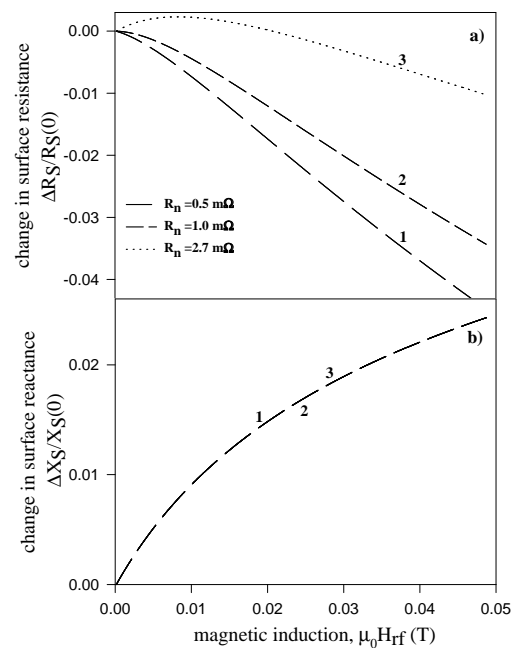


FIG. 3. $\Delta R_s(H)/R_s(0)$ and $\Delta X_s(H)/X_s(0)$ of the shunted weak link for different R_n values (given in the figures). Other parameters of the simulation are as follows: $f = 8 \cdot 10^9$ Hz; $\lambda_g(0) = 1.5 \cdot 10^{-7}$ m; $\rho_{s1}(0) = 2 \cdot 10^{-6}$ Ω·m; $J_{c0} = 1.1 \cdot 10^{10}$ A/m²; $H_J = 8 \cdot 10^3$ A/m; $H_g = 6.4 \cdot 10^6$ A/m; $d = 2 \cdot 10^{-8}$ m; $a = 3.6 \cdot 10^{-6}$ m.

are due to the non-monotonic field dependence of ρ_J . The latter, in turn, is due the size effect which arises when $\lambda_J(H)$, increasing with increased H , approaches the grain size, a . This effect is similar to the rf size-effect in thin metal plates¹⁸, though exact electrodynamics in this case is different. However, the non-monotonic behavior of both $R_s(H)$ and $X_s(H)$ in this geometry may be obtained only in the limit of $\omega l_J \gg \rho_J \gg \omega l_g$, which assures that both field-dependences of R_s and X_s of the structure are due to that of the junction resistivity. Bearing in mind that from physical considerations, such parameters as low power penetration depth, $\lambda_g(0)$ and the grain size, a are allowed to vary within rather narrow intervals ($130 \leq \lambda_g \leq 200$ nm, $0.1 \leq a \leq 10$ μm), we have to impose quite strict limitations on the value of other parameters, such as J_c and R_n . In fact, the limit $\omega l_J \gg \rho_J \gg \omega l_g$ can be well satisfied only for rather low- J_c junctions ($J_c \leq 10^5$ A/cm²), whereas reasonable values of ρ_J can be obtained for relatively low values of R_n ($0.1 \text{ m}\Omega \leq R_n \leq 10 \text{ m}\Omega$).

As far as the shunted WL geometry is concerned, the decrease in $R_s(H)$ arises due the current redistribution between the WL and the shunting grain. However, this may occur only in the limit when $\rho_J \gg \omega l_J \geq \omega l_g$, when an increase in ρ_J with increased H , forces the transport current to flow through the much less dissipative shunting grain, causing a reduction in the overall loss. At the same time, in the above limit, this geometry is incapable of producing a decrease in $X_s(H)$, since in this case the inductive response of the junction will always be governed by either $l_g(H)$, or the parallel combination of $l_g(H)$ and

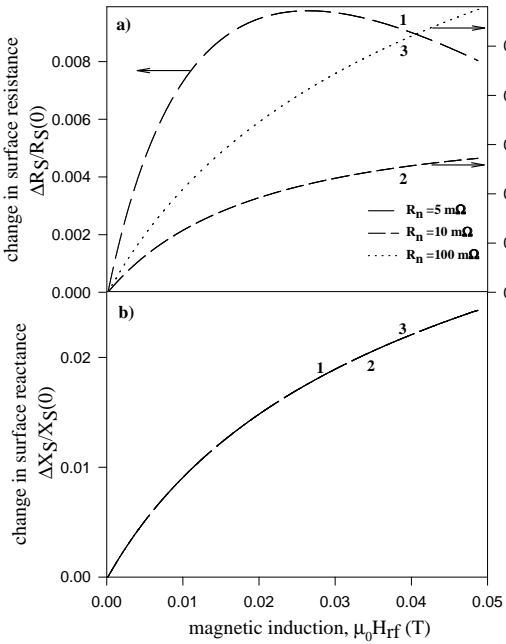


FIG. 4. The same data as in Fig.3, but for higher values of R_n (given in the figures). All other parameters are the same as in Fig.3.

$l_J(H)$, both of which are increasing functions of H . On the other hand, the opposite limit, $\omega l_J \gg \rho_J \gg \omega l_g$ will not give a decrease in $X_s(H)$ either, because of cancellation of the size-effect by the shunting grain.

It is worth noting that in this model the effects of anisotropy, relevant for the majority of HTS materials, have been ignored. However, preliminary investigation has shown that qualitatively the same features in $R_s(H)$ and $X_s(H)$ can be reproduced for rectangular grains with the anisotropy effects taken into account.

The model presented here was found to give a surprisingly good description of our own experimental results^{6,7,19} and those of others⁴. For instance, the geometry of the shunted WL, was found to give not only excellent qualitative agreement with our experiments on high-quality YBaCuO films, but very good quantitative agreement as well¹⁹. This encourages us to believe that the concepts contained within this model may reflect real physical processes occurring in HTS thin films in relatively low microwave and dc magnetic fields.

In conclusion, the magnetic field, H , dependence of the surface impedance, $Z_s = R_s + jX_s$, of a Josephson tunnel junction is simulated for two geometries; when the junction is shunted by another third grain, and for a non-shunted junction. In both cases, a non-monotonic behavior of $Z_s(H)$ is observed. In the case of the non-shunted junction, this arises due to the field-induced size effect in the weak link region with dimensions $a \sim \lambda_J$. In the shunted junction geometry, the observed decrease in $R_s(H)$ originates from the transport current redistribution between the weak link and the shunting grain. The model presented here gives rather good qualitative description of the unusual features in $Z_s(H)$, recently reported by some experimental groups^{4,6,7,19}. On the

other hand, this model is a simple alternative to other hypothetical explanations, like field-induced alignment of magnetic impurity spins⁹, or microwave stimulated superconductivity⁸, for which no rigorous theory of $Z_s(H)$ has yet been developed.

Further development of the model to include the case of Josephson junction arrays with a random distribution of the critical currents and dimensions, as well as an extension of the model for high dc fields, when the dissipation associated with the flux motion arises in grains, is expected.

I would like to greatly acknowledge fruitful clarifying discussions with C.E. Gough, A. M. Portis, A. Porch, M.A. Hein, J. Halbritter, J.C. Gallop and A.P. Kharel.

- ¹ P. P. Nguyen et al. , Phys. Rev. B **48** , 6400 (1993); D. E. Oates et al. , Phys. Rev. B **51** , 6686 (1995);
- ² S. Sridhar, Appl. Phys. Lett. **65**, 1054 (1994).
- ³ J. S. Herd, D. E. Oates, J. Halbritter, IEEE Trans. Appl. Supercond. **7**, 1299 (1997).
- ⁴ M. A. Hein et al. , J.Supercond. **10**, 485 (1997).
- ⁵ D. P. Choudhury, B. A. Willemsen, J. S. Derov and S. Sridhar, IEEE Trans. Appl. Supercond. **7**, 1260 (1997).
- ⁶ A. P. Kharel, A. V. Velichko, J. R. Powell, A. Porch, M. J. Lancaster et al. , Phys. Rev. B **58** , 11189 (1998).
- ⁷ A. Kharel et al. , IEEE Trans. Appl. Supercond. , in press.
- ⁸ G. M. Eliashberg, Sov. JETP Lett. **11**, 186 (1970).
- ⁹ Yu. N. Ovchinnikov and V. Z. Kresin, Phys. Rev. B **54**, 1251 (1996) and references therein.
- ¹⁰ J. C. Gallop, A. L. Cowie and L. F. Cohen, Proc. of EUCAS 1997, The Netherlands, **1**, 65 (1997).
- ¹¹ The idea of existence of the grain-shunted WLs in epitaxial HTS films was originally suggested by A. M. Portis et al. , Appl. Phys. Lett. **58**, 307 (1991).
- ¹² M. Tinkham and C. J. Lobb, in *Solid State Physics*, edited by H. Ehrenreich and D. Turnbull, (Academic Press, New York, 1989), Vol. 42, p. 91.
- ¹³ A. M. Portis, *Electrodynamics of High-Temperature Superconductors*, (World Scientific, Singapore, 1992).
- ¹⁴ J. Halbritter, J.Supercond. **8**, 690 (1995), and Ref.[12] therein.
- ¹⁵ T. van Duzer and C. W. Turner, *Principles of Superconducting Devices and Circuits*, (Elsevier, New York, 1991).
- ¹⁶ M. Mahel and J. Pivarc, Physica C **308**, 147 (1998).
- ¹⁷ In this limit, Eq.(2.7) is not strictly applicable due to inhomogeneity of the current distribution throughout the junction. However, we may use it, bearing in mind that the main feature produced by Eq.(7) is the non-monotonic behavior (size-effect) of $\rho_J(H)$, which will be inevitably present for $\lambda_J \sim a$, regardless of the particular form of $\rho_J(H)$.
- ¹⁸ S. Fahy, C. Kittel, and S. G. Louie, Am. J. Phys. **56**, 989 (1988).
- ¹⁹ A. V. Velichko et al. , to be published elsewhere.